Available online at www.sciencedirect.com
ScienceDirect
Journal of Molecular Catalysis A: Chemical 259 (2006) 150–155
JOURNAL OF MOLECULAR CATALYSIS A: CHEMICAL
www.elsevier.com/locate/molcata

Preparation of $H_3PMo_{12}O_{40}$ catalyst immobilized on surface modified mesostructured cellular foam (SM-MCF) silica and its application to the ethanol conversion reaction

Heesoo Kim [a], Ji Chul Jung [a], Pil Kim [a], Sung Ho Yeom [b], Kwan-Young Lee [c], In Kyu Song [a,*]

[a] *School of Chemical and Biological Engineering, Institute of Chemical Processes, Seoul National University, Shinlim-dong, Kwanak-ku, Seoul 151-744, South Korea*
[b] *Department of Environmental and Applied Chemical Engineering, Kangnung National University, Kangwondo 210-702, South Korea*
[c] *Department of Chemical and Biological Engineering, Korea University, Annam-dong, Sungbuk-ku, Seoul 136-701, South Korea*

Received 24 May 2006; accepted 13 June 2006
Available online 24 July 2006

Abstract

Surface of mesostructured cellular foam (MCF) silica was modified by grafting 3-aminopropyl-triethoxysilane (APTES) to have the positive charge, and thus, to provide sites for the immobilization of $H_3PMo_{12}O_{40}$. By taking advantage of the overall negative charge of $[PMo_{12}O_{40}]^{3-}$, $H_3PMo_{12}O_{40}$ catalyst was chemically immobilized on the aminopropyl group of surface modified MCF (SM-MCF) silica as a charge matching component. It was revealed that $H_3PMo_{12}O_{40}$ species were finely and molecularly dispersed on the SM-MCF silica via chemical immobilization. In the vapor-phase ethanol conversion reaction, the $H_3PMo_{12}O_{40}$/SM-MCF silica catalyst showed a higher ethanol conversion than the bulk $H_3PMo_{12}O_{40}$ catalyst. Furthermore, the $H_3PMo_{12}O_{40}$/SM-MCF silica catalyst exhibited an enhanced oxidation catalytic activity (formation of acetaldehyde) and a suppressed acid catalytic activity (formation of ethylene and diethylether) compared to the mother catalyst. The enhanced ethanol conversion and oxidation catalytic activity of $H_3PMo_{12}O_{40}$/SM-MCF silica catalyst was attributed to fine dispersion of $H_3PMo_{12}O_{40}$ species on the SM-MCF silica via chemical immobilization.

Keywords: Heteropolyacid catalyst; Mesostructured cellular foam silica; Immobilization; 3-Aminopropyl-triethoxysilane (APTES); Grafting; Vapor-phase ethanol conversion reaction

1. Introduction

Heteropolyacids (HPAs) have both acid and oxidation catalytic function [1–3], and therefore, they have been widely employed as homogeneous and heterogeneous catalysts for acid–base and oxidation reactions [4–9]. Tunable catalytic property of HPA catalysts depending on the identity of counter-cation [10], central heteroatom [11], and framework polyatom [12] is another great advantage for their successful catalytic applications.

One of the disadvantages of HPA catalysts, however, is that their surface area is very low (<10 m^2/g). To overcome the low surface area, HPA catalysts have been supported on inorganic mesoporous materials by a conventional impregnation method [13–15] or by a sol–gel synthesis method [16]. Another promising approach to enlarge the surface area of HPA catalysts is to take advantage of the overall negative charge of heteropolyanions. By this method, HPAs have been immobilized on ion-exchanged resins such as poly-4-vinylpyridine [17] or conjugated conducting polymers such as polyaniline [18]. However, such an attempt utilizing inorganic supporting materials has been restricted due to the difficulty in forming positive charge on the inorganic materials.

Mesoporous silicas have been synthesized from self-assembled aggregates of organic template and inorganic silica [19]. They have attracted much attention in many fields of science and engineering such as adsorption, separation, and catalysis [20–22], due to their unique pore structures. In particular, their remarkable textural properties such as high surface area and large pore volume make them well suitable for application

* Corresponding author. Tel.: +82 2 880 9227; fax: +82 2 888 7295.
E-mail address: inksong@snu.ac.kr (I.K. Song).

1381-1169/$ – see front matter © 2006 Elsevier B.V. All rights reserved.
doi:10.1016/j.molcata.2006.06.032

as catalyst supports. Thus, it is possible to design a catalyst that is homogeneously and molecularly dispersed in the pores of mesoporous silica. For this specific application, mesoporous silicas have been modified by introducing functional group such as terminal amine (–NH_2) and thiol (–SH) onto the surface through one-pot co-condensation [23,24] and post-modification methods [25]. Such a functionalized surface may provide anchoring sites for a certain catalyst, and therefore, a highly dispersed catalyst immobilized on the functionalized surface of mesoporous silica can be obtained.

In this work, mesostructured cellular foam (MCF) silica was prepared by a surfactant templating method. The surface of MCF silica was then modified by grafting 3-aminopropyl-triethoxysilane (APTES) to have the positive charge, and thus, to provide sites for the immobilization of $H_3PMo_{12}O_{40}$. By taking advantage of the overall negative charge of $[PMo_{12}O_{40}]^{3-}$, $H_3PMo_{12}O_{40}$ catalyst was chemically immobilized on the surface modified MCF (SM-MCF) silica as a charge matching component. The supported $H_3PMo_{12}O_{40}$/SM-MCF silica catalyst was applied to the vapor-phase ethanol conversion reaction. The catalytic performance of $H_3PMo_{12}O_{40}$/SM-MCF silica was then compared to that of the bulk $H_3PMo_{12}O_{40}$. It is known that ethylene and diethylether are formed by the acid catalytic function of HPA while acetaldehyde is produced by the oxidation catalytic function of HPA [3,5,6].

2. Experimental

2.1. Preparation of MCF silica

MCF silica was prepared according to the method in literature [26]. Four grams of PEO-PPO-PEO triblock copolymer (Pluronic P123 form BASF), an organic template, was dissolved in 150 ml of 1.6 M HCl solution at 35 °C. Four grams of 1,3,5-trimethylbenzene (TMB from Fluka), a swelling agent, was added into the solution containing the organic template. The mixed solution was then slowly added into 8.5 g of tetraethyl orthosilicate (TEOS from Fluka), a silica precursor. The resulting slurry was vigorously stirred at 35 °C for 24 h, and then it was maintained at 80 °C for 24 h. After the solid product was filtered and dried at room temperature, it was calcined at 550 °C for 5 h to yield the MCF silica.

2.2. Surface modification of MCF silica and immobilization of $H_3PMo_{12}O_{40}$

Fig. 1 shows the schematic procedures for the surface modification of MCF silica and the subsequent immobilization of $H_3PMo_{12}O_{40}$ (PMo_{12}) on the surface modified MCF (SM-MCF) silica. Surface modification of MCF silica was done by a grafting method [25]. A 0.26 ml of 3-aminopropyl-triethoxysilane (APTES from Aldrich) was slowly added into the dry toluene solution containing 1.5 g of MCF silica with constant stirring at room temperature under nitrogen atmosphere. After the solid product was filtered and dried, it was finally calcined at 180 °C for 2 h to yield the SM-MCF silica.

Immobilization of $H_3PMo_{12}O_{40}$ (PMo_{12} from Fluka) on the SM-MCF silica was achieved as following. SM-MCF silica (1.0 g) was added into the acetonitrile solution containing 0.5 g of PMo_{12} with vigorous stirring at room temperature, and the resulting solution was maintained at room temperature for 24 h. The solid product was filtered, and then it was dried overnight at 80 °C to yield the PMo_{12}/SM-MCF silica.

2.3. Characterization

Surface areas and pore volumes of MCF silica, SM-MCF silica, PMo_{12}/SM-MCF silica, and unsupported PMo_{12} samples were measured using an ASAP-2010 instrument (Micromeritics). To ensure the successful surface modification of MCF silica, nitrogen contents were determined by CHN elemental analyses (EC Instrument, EA1110). PMo_{12} content in the PMo_{12}/SM-MCF silica was measured by ICP-AES analysis (Shimadz, ICP-1000IV). Infrared spectra of the prepared samples were obtained with a FT-IR spectrometer (Nicolet, Impact 410). TGA analyses of SM-MCF silica, PMo_{12}/SM-MCF silica, and unsupported

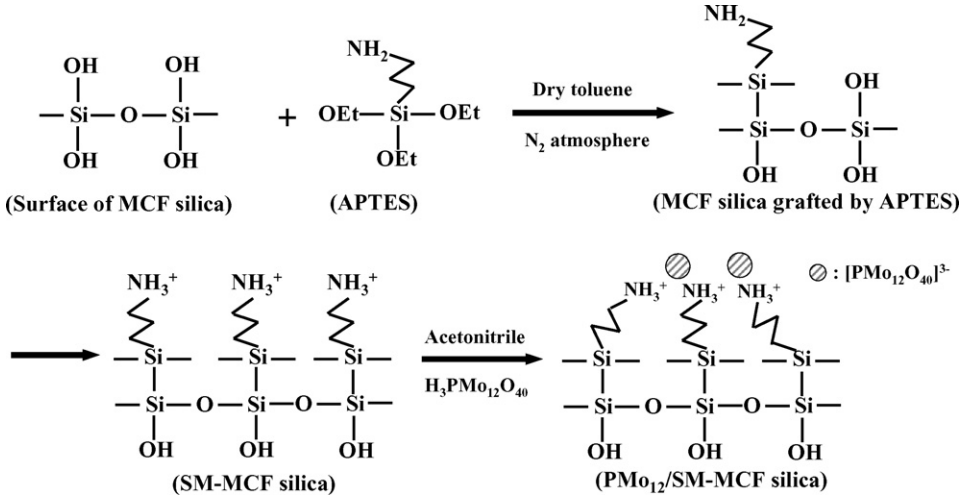

Fig. 1. Schematic procedures for the surface modification of MCF silica and the subsequent immobilization of $H_3PMo_{12}O_{40}$ (PMo_{12}) on the surface modified MCF (SM-MCF) silica.

Table 1
Physical properties of supports and catalysts

	BET surface area (m^2/g)	Pore volume (cm^3/g)	Nitrogen content (wt%)	PMo_{12} content (wt%)
MCF silica	621	1.18	0	–
SM-MCF silica	410	0.89	1.07	–
PMo_{12}/SM-MCF silica	210	0.49	0.90	10.7
Unsupported PMo_{12}	8	–	–	–

PMo_{12} samples were conducted using a TGA-50 instrument (Shimadz) in an air stream at a heating rate of 5 °C/min. Crystal state of PMo_{12} in the PMo_{12}/SM-MCF silica was confirmed by XRD measurement (MAC Science, M18XHF-SRA).

2.4. Vapor-phase ethanol conversion reaction

Vapor-phase ethanol conversion reaction was carried out in a continuous flow fixed-bed reactor at an atmospheric pressure. PMo_{12}/SM-MCF silica or unsupported PMo_{12} (120 mg on PMo_{12} basis) was charged into a tubular quartz reactor, and it was pretreated with an air stream (20 ml/min) at 250 °C for 2 h. Ethanol (3.43×10^{-3} mol/h) was sufficiently vaporized by passing a preheating zone and fed into the reactor continuously together with air stream (20 ml/min). Contact time was maintained at 35.0 g-PMo_{12}-h/ethanol-mole. The catalytic reaction was carried out at 230 °C for 5 h. Reaction products were periodically sampled and analyzed with a gas chromatography (HP 5890 II).

3. Results and discussion

3.1. Physical properties of supports and catalysts

Table 1 shows the physical properties of supports and catalysts. BET surface areas and pore volumes were decreased in the order of MCF silica > SM-MCF silica > PMo_{12}/SM-MCF silica. Surface area of MCF silica was decreased after surface modification step due to the successful grafting of APTES. Furthermore, PMo_{12}/SM-MCF silica showed a lower surface area than SM-MCF silica due to the immobilization of PMo_{12}. However, PMo_{12}/SM-MCF silica catalyst still retained relatively high surface area and large pore volume. The amounts of aminopropyl functional group in SM-MCF silica and PMo_{12}/SM-MCF silica were indirectly measured by determining the nitrogen contents. Nitrogen contents in SM-MCF silica and PMo_{12}/SM-MCF silica were determined to be 1.07 and 0.90 wt%, respectively, while no nitrogen was detected in pure MCF silica. The amount of PMo_{12} immobilized on PMo_{12}/SM-MCF silica was found to be 10.7 wt%. We also attempted to immobilize PMo_{12} on pure MCF silica. In this case, however, PMo_{12} species were totally dissolved out during the washing step due to the absence of anchoring sites for PMo_{12} in the pure MCF silica. The above results imply that aminopropyl functional group in the SM-MCF silica played a key role for the immobilization of PMo_{12}.

Fig. 2 shows the TEM images of MCF silica, SM-MCF silica, and PMo_{12}/SM-MCF silica. Pore walls of SM-MCF silica and PMo_{12}/SM-MCF silica were slightly agglomerated by APTES, compared to those of pure MCF silica. However, disordered pore arrays of MCF silica were clearly observed in all samples. Pore diameters of these samples determined from TEM images were ca. 20 nm with no great difference.

3.2. Chemical immobilization of $H_3PMo_{12}O_{40}$ on SM-MCF silica

Successful immobilization of PMo_{12} on the SM-MCF silica was confirmed by FT-IR analyses as shown in Fig. 3. The Si–O–Si stretching bands originated from MCF silica were observed at around 1250–1000, 800, and 475 cm^{-1}. A weak band at around 1500 cm^{-1} observed in SM-MCF silica and PMo_{12}/SM-MCF silica was attributed to $-NH_3^+$ stretching vibration, indicating the presence of aminopropyl functional group in these two samples. The primary structure of bulk PMo_{12} could be identified by four characteristic IR bands appearing at 1064 cm^{-1} (P–O band), 964 cm^{-1} (Mo=O band), 868

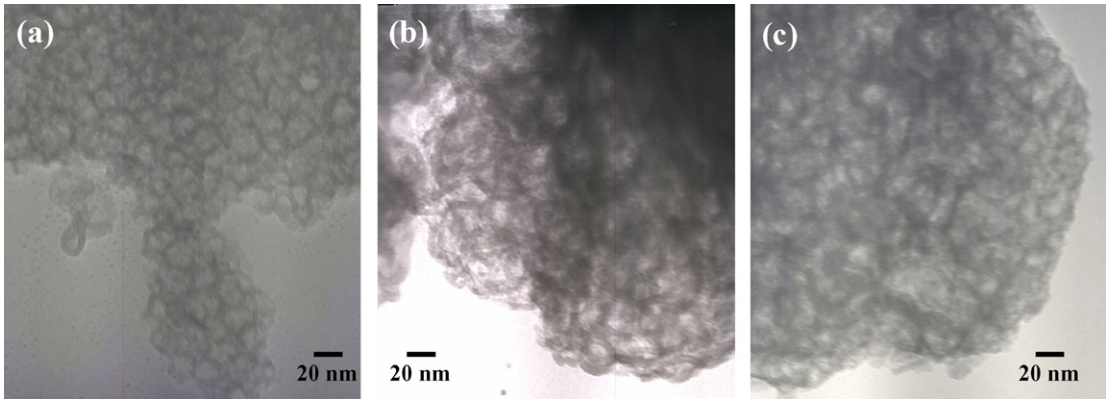

Fig. 2. TEM images of (a) MCF silica, (b) SM-MCF silica, and (c) PMo_{12}/SM-MCF silica.

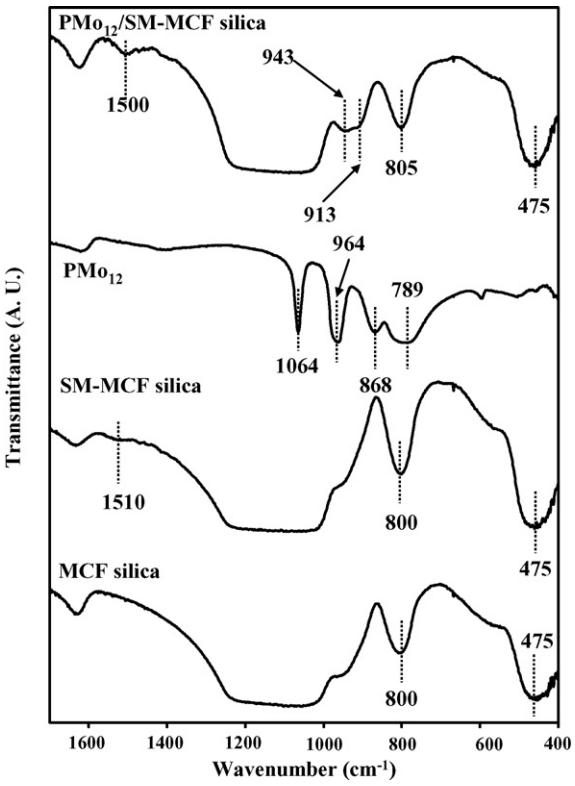

Fig. 3. FT-IR spectra of MCF silica, SM-MCF silica, bulk PMo_{12}, and PMo_{12}/SM-MCF silica.

and 789 cm^{-1} (Mo–O–Mo bands) [6,27]. The characteristic IR bands of PMo_{12} in the PMo_{12}/SM-MCF silica were somewhat different from those of unsupported PMo_{12}. The P–O band in the PMo_{12}/SM-MCF silica was not clearly identified due to the overlap by the broad Si–O–Si band. However, Mo=O and Mo–O–Mo bands of PMo_{12} in the PMo_{12}/SM-MCF silica appeared at shifted positions compared to those of unsupported PMo_{12}, indicating a strong chemical interaction between PMo_{12} and SM-MCF silica [18,27]. It is inferred that aminopropyl functional group of SM-MCF silica with terminal $–NH_3^+$ served as an anchoring site for $[PMo_{12}O_{40}]^{3-}$.

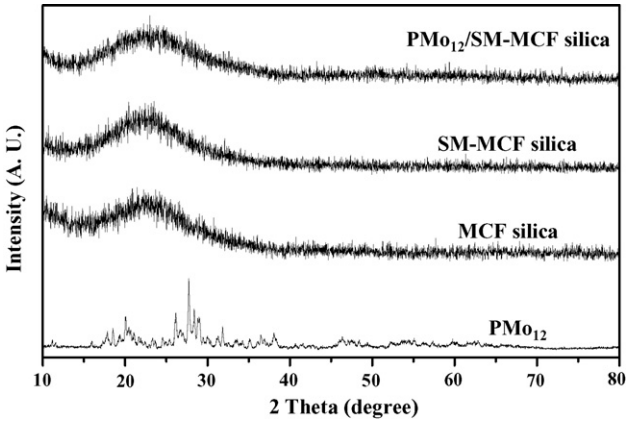

Fig. 4. XRD patterns of bulk PMo_{12}, MCF silica, SM-MCF silica, and PMo_{12}/SM-MCF silica.

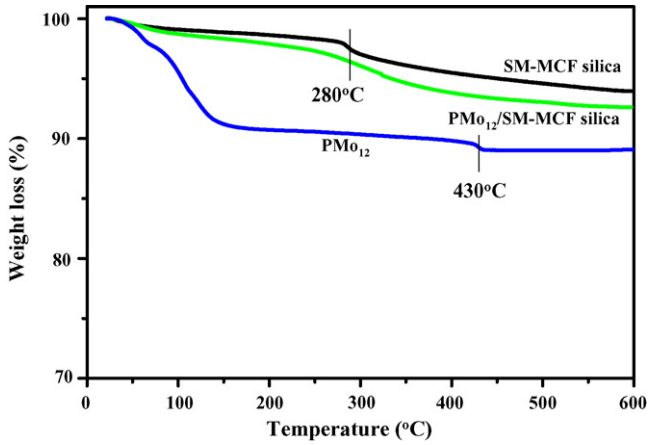

Fig. 5. TGA profiles of bulk PMo_{12}, SM-MCF silica, and PMo_{12}/SM-MCF silica.

Fig. 4 shows the XRD patterns of bulk PMo_{12}, MCF silica, SM-MCF silica, and PMo_{12}/SM-MCF silica. Unsupported PMo_{12} catalyst showed a characteristic XRD pattern of the HPA. On the other hand, MCF silica and SM-MCF silica showed no characteristic XRD patterns due to their amorphous nature. It is noticeable that PMo_{12}/SM-MCF silica also showed no characteristic XRD pattern, even though 10.7 wt% PMo_{12} was loaded on the SM-MCF silica. This result means that PMo_{12} species were not in a crystal phase but in an amorphous-like state, demonstrating that PMo_{12} species with a molecular size of ca. 1 nm were finely and molecularly dispersed on the SM-MCF silica via chemical immobilization.

3.3. Thermal stability of SM-MCF silica and PMo_{12}/SM-MCF silica

Fig. 5 shows the TGA profiles of bulk PMo_{12}, SM-MCF silica, and PMo_{12}/SM-MCF silica. Thermal scanning was done from room temperature to 600 °C in an air stream. Bulk PMo_{12} catalyst experienced significant weight loss at low temperature region (<150 °C) due to the removal of crystalline water molecules, and then it was finally decomposed at 430 °C [6,11]. The weight loss of SM-MCF silica and PMo_{12}/SM-MCF silica below 280 °C was less than 3 wt%, which was attributed to the removal of small amounts of physically adsorbed water and residual solvent. The weight loss of SM-MCF silica and PMo_{12}/SM-MCF silica above 280 °C was believed to be due to the decomposition of aminopropyl functional group. This means that SM-MCF silica and PMo_{12}/SM-MCF silica are thermally stable at temperatures below 280 °C. It is expected that PMo_{12}/SM-MCF silica can be utilized as a finely and molecularly dispersed PMo_{12} catalyst for the catalytic reactions performed below 280 °C.

3.4. Catalytic performance of PMo_{12}/SM-MCF silica in the ethanol conversion reaction

Fig. 6 shows the ethanol conversions over bulk PMo_{12} and PMo_{12}/SM-MCF silica catalysts at 230 °C. The PMo_{12}/SM-MCF silica catalyst exhibited a remarkably enhanced ethanol

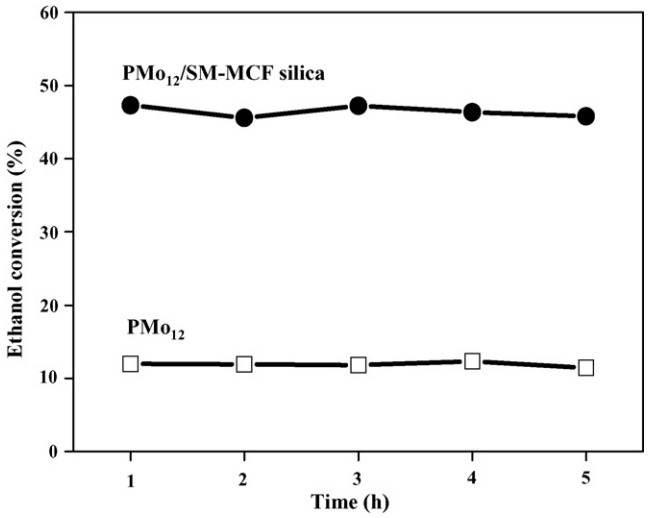

Fig. 6. Ethanol conversions over bulk PMo_{12} and PMo_{12}/SM-MCF silica catalysts at 230 °C.

conversion compared to the unsupported PMo_{12} catalyst. The enhanced ethanol conversion of PMo_{12}/SM-MCF silica catalyst was attributed to finely and molecularly dispersed PMo_{12} species on the SM-MCF silica support.

Fig. 7 shows the product selectivities over bulk PMo_{12} and PMo_{12}/SM-MCF silica catalysts at 230 °C. In the catalytic reaction, negligible amounts of CO, CO_2, and butanol were detected as by-products. It is known that ethylene and diethylether are formed by the acid catalytic function of HPA while acetaldehyde is produced by the oxidation catalytic function of HPA [3,5,6]. What is noticeable is that the PMo_{12}/SM-MCF silica catalyst exhibited a remarkably enhanced oxidation catalytic activity (formation of acetaldehyde) and a suppressed acid catalytic activity (formation of ethylene and diethylether) compared to the mother catalyst. Unsupported PMo_{12} catalyst retains its own acid and oxidation catalytic function. Unlike the bulk PMo_{12}, PMo_{12} catalyst in the PMo_{12}/SM-MCF silica was chemically immobilized on the positive site ($–NH_3^+$) of SM-MCF silica

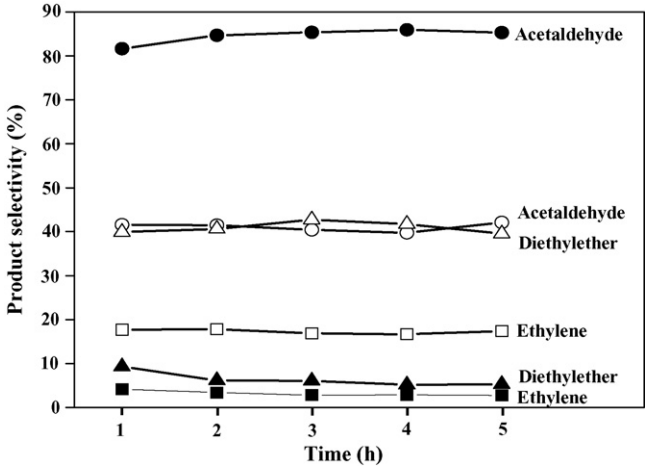

Fig. 7. Product selectivities over bulk PMo_{12} and PMo_{12}/SM-MCF silica catalysts at 230 °C: (closed symbol) PMo_{12}/SM-MCF silica, and (open symbol) unsupported PMo_{12}.

by losing proton. As attempted in this work, it is believed that $[PMo_{12}O_{40}]^{3-}$ species were finely and chemically immobilized on the SM-MCF silica as charge matching components by losing protons (acid sties). Therefore, the PMo_{12}/SM-MCF silica catalyst showed an enhanced oxidation catalytic activity and a suppressed acid catalytic activity compared to the mother catalyst.

4. Conclusions

MCF silica was prepared by a surfactant templating method. The surface of MCF silica was then modified by grafting 3-aminopropyl-triethoxysilane (APTES) to have the positive charge, and thus, to provide sites for the immobilization of PMo_{12}. By taking advantage of the overall negative charge of $[PMo_{12}O_{40}]^{3-}$, PMo_{12} catalyst was chemically immobilized on the SM-MCF silica as a charge matching component. It was revealed that PMo_{12} species were finely and molecularly dispersed on the SM-MCF silica via chemical immobilization. In the vapor-phase ethanol conversion reaction, the PMo_{12}/SM-MCF silica catalyst showed a remarkably enhanced ethanol conversion compared to the unsupported PMo_{12} catalyst. The enhanced ethanol conversion of PMo_{12}/SM-MCF silica catalyst was due to finely and molecularly dispersed PMo_{12} species on the SM-MCF silica support. Moreover, the PMo_{12}/SM-MCF silica catalyst exhibited a remarkably enhanced oxidation catalytic activity (formation of acetaldehyde) and a suppressed acid catalytic activity (formation of ethylene and diethylether) compared to the mother catalyst. The enhanced oxidation catalytic activity and the suppressed acid catalytic activity of PMo_{12}/SM-MCF silica was attributed to finely and molecularly dispersed PMo_{12}, which was chemically immobilized on the positive site ($–NH_3^+$) of SM-MCF silica by sacrificing its proton (Brönsted acid site).

Acknowledgement

The authors acknowledge the support from Korea Science and Engineering Foundation (KOSEF R01-2004-000-10502-0).

References

[1] M.T. Pope, Heteropoly and Isopoly Oxometalates, Springer-Verlag, New York, 1983.
[2] J.B. McMonagle, J.B. Moffat, J. Catal. 91 (1985) 132.
[3] M. Misono, Catal. Rev. Sci. Eng. 29 (1987) 199.
[4] C.L. Hill, C.M. Prosser-McCartha, Coord. Chem. Rev. 143 (1995) 407.
[5] I.V. Kozhevnikov, Catal. Rev. Sci. Eng. 37 (1995) 311.
[6] T. Okuhara, N. Mizuno, M. Misono, Adv. Catal. 41 (1996) 113.
[7] I.K. Song, S.H. Moon, W.Y. Lee, Korean J. Chem. Eng. 8 (1991) 33.
[8] I.K. Song, M.A. Barteau, Korean J. Chem. Eng. 19 (2002) 567.
[9] I.K. Song, H.S. Kim, M.-S. Chun, Korean J. Chem. Eng. 20 (2003) 844.
[10] M. Ai, J. Catal. 71 (1981) 88.
[11] M.H. Youn, H. Kim, J.C. Jung, I.K. Song, K.P. Barteau, M.A. Barteau, J. Mol. Catal. A 241 (2005) 227.
[12] I.K. Song, M.A. Barteau, J. Mol. Catal. A 212 (2004) 229.
[13] W. Chu, X. Yang, Y. Shan, X. Ye, Y. Wu, Catal. Lett. 42 (1996) 201.
[14] K. Nowinska, R. Formaniak, W. Kaleta, A. Waclaw, Appl. Catal. A 256 (2003) 115.
[15] N.-Y. He, C.-S. Woo, H.-G. Kim, H.-I. Lee, Appl. Catal. A 281 (2005) 167.

[16] A. Lapkin, B. Bozkaya, T. Mays, L. Borello, K. Edler, B. Crittenden, Catal. Today 81 (2003) 611.
[17] K. Nomiya, H. Murasaki, M. Miwa, Polyhedron 5 (1986) 1031.
[18] M. Hasik, W. Turek, E. Stochmal, M. Lapowski, A. Proń, J. Catal. 147 (1994) 544.
[19] C.T. Kresge, M.E. Leonowicz, W.J. Roth, J.C. Vartuli, J.S. Beck, Nature 359 (1992) 710.
[20] M.E. Davis, Nature 417 (2002) 813.
[21] A. Stein, Adv. Mater. 15 (2003) 763.
[22] T. Kang, Y. Park, J. Yi, Ind. Eng. Chem. Res. 43 (2004) 1478.
[23] X. Wang, K.S.K. Lin, J.C.C. Chan, S. Cheng, J. Phys. Chem. B 109 (2005) 1763.
[24] A.S.M. Chong, X.S. Zhao, J. Phys. Chem. B 107 (2003) 12650.
[25] A.R. Cestari, E.F.S. Vieira, E.S. Silva, J. Colloid Interface Sci. 297 (2006) 22.
[26] D. Zhao, J. Feng, Q. Huo, N. Melosh, G.H. Fredrickson, B.F. Chmelka, G.D. Stucky, Science 279 (1998) 548.
[27] H. Kim, P. Kim, K.-Y. Lee, S.H. Yeom, J. Yi, I.K. Song, Catal. Today 111 (2006) 361.